

# 1 Capillary Trapping of CO<sub>2</sub> in Oil Reservoirs: 2 Observations in a Mixed-wet Carbonate Rock

3 *Ali S. Al-Menhali\**, *Samuel Krevor*

4 Qatar Carbonates and Carbon Storage Research Centre, Department of Earth Science and  
5 Engineering, Imperial College London, London SW7 2AZ, U.K.

6

## 7 KEYWORDS

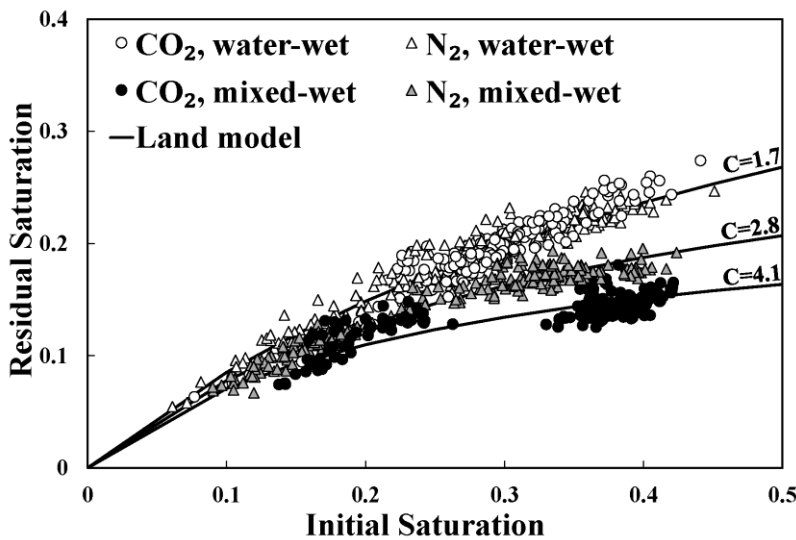
8 Residual trapping, capillary trapping, remaining saturations, mixed-wet, supercritical CO<sub>2</sub>, CCS,  
9 EOR, X-ray, carbon utilization.

10

## 11 ABSTRACT

12 Early deployment of carbon dioxide storage is likely to focus on injection into mature oil  
13 reservoirs, most of which occur in carbonate rock units. Observations and modeling have shown  
14 how capillary trapping leads to the immobilization of CO<sub>2</sub> in saline aquifers, enhancing the security  
15 and capacity of storage. There are, however, no observations of trapping in rocks with a mixed-  
16 wet state characteristic of hydrocarbon bearing carbonate reservoirs. Here we found that residual  
17 trapping of supercritical CO<sub>2</sub> in a limestone altered to a mixed-wet state with oil was significantly

18 less than trapping in the unaltered rock. In unaltered samples, the trapping of CO<sub>2</sub> and N<sub>2</sub> were  
19 indistinguishable, with a maximum residual saturation of 24%. After altering the wetting state, the  
20 trapping of N<sub>2</sub> was reduced, with a maximum residual saturation of 19%. The trapping of CO<sub>2</sub> was  
21 reduced even further with a maximum residual saturation of 15%. Best fit Land model constants  
22 shifted from  $C = 1.73$  in the water-wet rock, to  $C = 2.82$  for N<sub>2</sub>, and  $C = 4.11$  for the CO<sub>2</sub> in the  
23 mixed-wet rock. The weakened trapping indicates that plume migration will be farther and the  
24 timescales for immobilization will be longer for CO<sub>2</sub> storage projects using oil fields compared  
25 with saline aquifers.



26

27

## 28 INTRODUCTION

29 The capture of carbon dioxide emitted from industrial processes and subsequent storage in  
30 subsurface geologic units has been identified as a key technology in the global reduction of  
31 anthropogenic CO<sub>2</sub> emissions to the atmosphere<sup>1</sup>. Capillary trapping, also called residual  
32 trapping, is one of the most significant physical mechanisms ensuring the permanence of CO<sub>2</sub>

33 storage in the subsurface<sup>1,2</sup>. Capillary trapping limits the extent of CO<sub>2</sub> migration<sup>3,4</sup>, underpins  
34 estimates of regional storage capacity<sup>5-8</sup> and controls the movement of the mobile sections of a  
35 subsurface plume through its relationship with fluid flow property hysteresis<sup>4,9,10</sup>. Thus a  
36 significant body of recent work has focused on observations characterizing capillary trapping<sup>2</sup>,  
37 including in carbonate rocks<sup>11</sup>.

38 Saline aquifer storage presents the largest potential for global CO<sub>2</sub> storage capacity<sup>12</sup> and the  
39 focus of the previous observations has been on the characterization of rocks unaltered by  
40 hydrocarbons. On the other hand, oil fields have a number of characteristics that could lead to  
41 their having an outsized importance during the early deployment of carbon storage. Commercial  
42 oil fields are well characterized, have a demonstrated fluid trap, and sometimes have  
43 infrastructure that can be repurposed for use with CO<sub>2</sub> injection<sup>13,14</sup>. Enhanced oil recovery with  
44 CO<sub>2</sub> injection may also provide for a significant revenue stream. These benefits are reflected in  
45 the dominance of enhanced oil recovery in the current portfolio of existing industrial scale  
46 sequestration projects<sup>15</sup>.

47 The capillary properties of rocks typical of saline aquifer systems - unaltered by hydrocarbons  
48 - are considered water-wet with respect to CO<sub>2</sub>-brine systems across wide range of reservoir  
49 conditions<sup>16</sup>, although some important questions remain including the impact of chemical  
50 process kinetics on the wetting state<sup>17,18</sup>. In contrast, hydrocarbon reservoirs are characterized by  
51 a mixed-wet state, wherein chemical deposits from the hydrocarbon phase onto the surface of the  
52 pore mineral surfaces over geologic time have resulted in connected oil-wetting conduits to  
53 flow<sup>19</sup>. This has a significant impact on the flow properties of the system, including the capillary  
54 pressure, relative permeability, and residual trapping characteristic functions<sup>20-22</sup>.

55 Of key importance for the security of CO<sub>2</sub> storage is that the capillary trapping of nonpolar  
56 fluids, like CO<sub>2</sub>, have been observed to be significantly less in mixed wet rocks than trapping in  
57 water wet rocks typical of saline aquifers<sup>23-25</sup>. This issue has been largely ignored in the flow  
58 modelling literature for CO<sub>2</sub> storage and there are no observations characterizing the extent of  
59 capillary trapping that will take place with CO<sub>2</sub> in mixed-wet rocks. In this work we provide the  
60 first observations that a key trapping mechanism underpinning the security of CO<sub>2</sub> storage is  
61 significantly reduced in the very storage locations that are among the most economically  
62 appealing for the first generation of project development.

63 The key aim of this study was to evaluate the impact of the wetting state typical of carbonate  
64 oil reservoirs on trapping for CO<sub>2</sub> storage. We have done this by characterizing the trapping of  
65 supercritical CO<sub>2</sub> in a mixed-wet carbonate rock, comparing this with the degree of trapping in  
66 the same rock prior to alteration to the mixed wet state. We focused on a carbonate rock because  
67 of the prevalence of carbonate lithology in oil production<sup>26,27</sup>. To isolate the effects of wetting  
68 alteration from fluid-rock chemical reaction and mass transfer, the CO<sub>2</sub> and brine were  
69 equilibrated together with crushed samples of the rock prior to observations of trapping.  
70 Experiments were also performed with N<sub>2</sub> –water systems in unaltered and altered samples as a  
71 benchmark for comparison.

72

## 73 MATERIALS

74 **Rock Samples, Fluids, and Test Conditions.** A total of 14 core flood experiments were  
75 carried out on two Estailades limestone core samples before and after alteration with a

76 hydrocarbon mixture. The sequence of experiments, fluid pairs, and drainage flow rates are  
77 provided in Table 1.

78 Estailades is a quarry carbonate limestone from the Estailade Formation located in southeast  
79 France<sup>28</sup>. The sample consists of 97.9% calcite and 2.1% quartz, measured by Weatherford  
80 Laboratories, East Grinstead, UK. The faces of the core were machined flat to ensure contact with  
81 the end-caps. Each sample was vacuum dried at 70 °C overnight before each test.

82 A single sample, E1, was used to compare trapping between water-wet and mixed-wet  
83 systems. Observations were first made on the sample unaltered by hydrocarbon, and again after  
84 altering the wetting state to a mixed-wet state using a procedure described in more detail below.  
85 A second sample, E2, was used for a reproduction of observations in the unaltered rock. Both  
86 samples were 3.8 cm in diameter and 12 cm in length. The absolute permeability of the E1 and  
87 E2 samples to water were 138 and 148 mD, respectively. The average porosities as measured  
88 with X-ray computed tomography (CT) were 28 and 29% for the E1 and E2 samples,  
89 respectively.

90 Carbon dioxide and nitrogen were used as the non-polar fluid phases in the core-flooding  
91 experiments, both with 99.9% purity (BOC Industrial Gases, UK). Nitrogen was used as the  
92 benchmark nonwetting phase primarily because the thermophysical properties, including the  
93 wetting state in unaltered carbonate rocks, was well constrained. There were other considerations  
94 – the viscosity of N<sub>2</sub> is more similar to that of CO<sub>2</sub> than a typical benchmark hydrocarbon liquid  
95 like decane. The use of N<sub>2</sub> allowed us to perform experiments in sequences alternating fluid pairs  
96 without the need for a solvent based cleaning of the rock core, a process which may have altered  
97 the wetting state and put further stress on the rock. The aqueous phase fluids used were

98 deionized water or brine consisting of deionized water and NaCl with total salt molality of 1 mol  
 99 kg<sup>-1</sup>. Arabian Medium crude oil (API=30.77°) and heptane with 99% purity (Sigma-Aldrich)  
 100 were used for the wettability alteration and Amott tests<sup>29</sup>. Toluene with 99.8% purity (Sigma-  
 101 Aldrich) was used as a solvent in the filtration experiments made prior wetting alteration to  
 102 measure asphaltene precipitation of the crude oil.

103 All core flooding experiments were performed at 10 MPa pore pressure. The CO<sub>2</sub>-brine  
 104 experiments were performed at a temperature of 50 °C while N<sub>2</sub>-water experiments were at 25  
 105 °C. The thermophysical properties of the fluids are provided as follows: The interfacial tension  
 106 value of CO<sub>2</sub> and brine at the experimental condition was estimated to be 37 mN/m<sup>30</sup> while N<sub>2</sub>  
 107 and water interfacial tension value was 67 mN/m<sup>31</sup>. The CO<sub>2</sub>/brine and N<sub>2</sub>/water viscosities were  
 108 estimated to be 0.03/0.61 and 0.02/0.89 cP, respectively<sup>32,33</sup>. The CO<sub>2</sub>/brine and N<sub>2</sub>/water  
 109 densities were estimated to be 0.39/1.02 and 0.11/1.01 g/cm<sup>3</sup>, respectively<sup>33</sup>.

110 **Table 1.** Initial-residual core flooding experiments and repeats in the chronological sequence  
 111 that they were performed.

Experiment number <sup>a</sup>	Sample name / wetting state	Fluid pairs	Drainage flow rate <sup>b</sup> [ml min <sup>-1</sup> ]	Pore volumes injected during imbibition
1	E1 / water-wet	<i>N<sub>2</sub> / water</i>	0.5	0.25
2	E1 / water-wet	<i>N<sub>2</sub> / water</i>	20	0.17
3	E1 / water-wet	<i>N<sub>2</sub> / water</i>	- <sup>c</sup>	0.63
4a	E1 / mixed-wet	<i>N<sub>2</sub> / water</i>	20	0.2
5a	E1 / mixed-wet	<i>N<sub>2</sub> / water</i>	0.5	0.36
6a	E1 / mixed-wet	<i>CO<sub>2</sub> / brine</i>	20	0.2
7	E1 / mixed-wet	<i>CO<sub>2</sub> / brine</i>	0.5	0.63
4b	E1 / mixed-wet	<i>N<sub>2</sub> / water</i>	20	1.29
5b	E1 / mixed-wet	<i>N<sub>2</sub> / water</i>	0.5	1.71
8	E2 / water-wet	<i>N<sub>2</sub> / water</i>	20	0.45
9a	E2 / water-wet	<i>CO<sub>2</sub> / brine</i>	20	0.44

9b	E2 / water-wet	<i>CO<sub>2</sub> / brine</i>	20	0.98
10	E2 / water-wet	<i>CO<sub>2</sub> / brine</i>	0.5	0.23
6b	E1 / mixed-wet	<i>CO<sub>2</sub> / brine</i>	20	0.23

112 <sup>a</sup> Experiments with a common number indicate repeat tests on the same sample, at the same wetting state, and  
113 fluid flow condition, i.e., test 4b is a repeat of test 4a, but after the rock core has been exposed to CO<sub>2</sub> during tests 6a  
114 and 7.

115 <sup>b</sup> Imbibition was at 0.5 ml min<sup>-1</sup> for all experiments

116 <sup>c</sup> Experiment 3 was initially fully saturated with N<sub>2</sub> instead of water. Water was subsequently injected at 0.5 ml  
117 min<sup>-1</sup> to measure the initial-residual relationship at 100% initial gas saturation

118 **Core-flooding Experimental Setup.** Residual trapping measurements were conducted using a  
119 two fluid phase core flooding system described in detail in previous papers by the authors<sup>16</sup>. The  
120 experimental setup was designed to maintain temperature and pressure conditions of up to 120 °C  
121 and 30 MPa. The system was modified for experiments with carbonates samples and included a  
122 stirred reactor to equilibrate fluids with ground sample of the solid (Parr Instruments Co., IL,  
123 USA). A schematic is provided in the supporting information.

124

## 125 METHOD

126 **Core-flooding Test and Sequence.** A core flooding technique<sup>34</sup> was applied in this work for  
127 the construction of initial-residual characteristic trapping curves. The technique combines the  
128 deliberate creation of capillary pressure gradients in the core with in-situ saturation monitoring to  
129 rapidly construct the initial-residual curve across a range of saturations. A detailed description of  
130 the startup and operation of the experiment is provided in the supporting information and  
131 summarized here.

132 To create the initial saturation, a primary drainage step was performed, injecting CO<sub>2</sub> or N<sub>2</sub> at a  
133 constant rate of either 0.5 or 20 ml min<sup>-1</sup> into an initially water or brine-saturated core sample,  
134 Table 1. The choice of flow rate was made at different stages in the experiment to cover a particular  
135 range of the initial-residual curves – larger flow velocities during drainage result in larger initial  
136 saturations. X-ray scans were then performed to evaluate the initial saturation along the length of  
137 the rock core. Imbibition was then performed by injecting brine or water, pre-equilibrated with  
138 CO<sub>2</sub> and the limestone sample, at 0.5 ml min<sup>-1</sup>. Saturations were calculated at each stage with X-  
139 ray CT using the standard approach<sup>35</sup> detailed in the supporting information. Several scans were  
140 taken to confirm measurements of imbibition and to reduce the uncertainty associated with the  
141 computed saturations.

142 To minimize the impact of calcite in the rock dissolving into the acidified brine, the brine was  
143 pre-equilibrated with both CO<sub>2</sub> and the rock material at the experimental conditions prior to the  
144 residual trapping test. The fluids were mixed vigorously together with crushed grains of the same  
145 rock in a Parr stirred reactor at experimental conditions for 24 hrs. Then, this CO<sub>2</sub> and brine were  
146 co-circulated at experimental conditions in a closed loop bypassing the core, but including  
147 circulation through the reactor. The dissolution of CO<sub>2</sub> into water was monitored by observing the  
148 volume balance of the fluid phases in the closed loop, maintained at constant pressure. X-ray  
149 imaging was used to confirm that the porosity was not changing during the tests. A comparison of  
150 the repeatability of the results of N<sub>2</sub> tests before and after CO<sub>2</sub> flooding tests also supported the  
151 view that the rock core, and its wetting state, were not significantly altered by the exposure to CO<sub>2</sub>.  
152 The absolute permeability to water was measured before each experiment and varied less than 4%  
153 throughout the series of tests suggesting minimal changes in the pore structure of the core sample  
154 throughout the entire course of experiments. The slice average porosity along the entire length of



155 core was also measured at a resolution of 1 mm after each test with X-ray scanning providing  
156 another confirmation that rock properties were not significantly altered.

157 The sequence of tests were designed to test the impact of altering the wetting state and confirm  
158 that variations in observations were due to the change in wetting state. See Table 1. Tests 1-3 were  
159 used to construct the initial-residual curve for sample E1 using N<sub>2</sub> with the rock in the natural state,  
160 unaltered by hydrocarbon. The wetting state was altered as described below and subsequent tests  
161 characterizing the initial-residual curve were performed first using the N<sub>2</sub>-water system (tests 4a,  
162 5a) and then the CO<sub>2</sub>-brine system (tests 6a, 7). Repeat tests were then performed with N<sub>2</sub> (tests  
163 4b, 5b) to assess the impact, if any, of CO<sub>2</sub> exposure to the altered wetting state. A final repeat test  
164 was performed with CO<sub>2</sub> (6b) to test repeatability of the residual trapping at high initial saturation  
165 with CO<sub>2</sub>.

166 At the outset of the study, we hypothesized that the N<sub>2</sub>-brine and CO<sub>2</sub>-brine initial-residual  
167 curves would match based on previous experience<sup>34</sup>. As will be discussed in the results, this turned  
168 out not to be the case for the initial residual curves obtained after altering the rock with  
169 hydrocarbon. To ensure that this effect was a result of the wetting state change, and not the  
170 propagation of a feature of CO<sub>2</sub> and N<sub>2</sub> trapping in unaltered carbonates, another set of tests was  
171 performed on a second sample of unaltered Estailades rock comparing N<sub>2</sub> and CO<sub>2</sub> trapping, tests  
172 8-10.

173 Injected pore volumes were kept to a minimum due to the corrosive nature of the fluids and the  
174 relative fragility of the rock under the test conditions. This is a particular difficulty of scientific  
175 studies using reservoir condition core floods – a single rock sample must endure a sequence of  
176 tests which place significant stress on the rock. In water wet systems, a single pore volume is

177 sufficient to achieve the residual saturation<sup>34</sup>, whereas hundreds or even thousands of injected pore  
178 volumes are required to achieve the true residual in mixed-wet systems<sup>24</sup>. In both water-wet and  
179 mixed-wet systems there is an initial rapid desaturation of the non-wetting phase with less than  
180 one pore volume of fluid injected. In the mixed-wet case, however, this is followed by a very slow  
181 rate of desaturation during subsequent brine injection. In the tests performed in this work, the  
182 initial rapid desaturation was monitored using X-ray scanning. The point of comparison of the  
183 initial-residual curves was made using saturation measurements obtained following this initial  
184 phase of rapid desaturation, generally between 0.25 and 1.5 pore volumes of brine injected, Table  
185 1. The saturation of CO<sub>2</sub> in a mixed-wet system after such volumes of imbibition will be similar  
186 to saturations in a field setting far from the well where the CO<sub>2</sub> has been injected. However, the  
187 ultimate residual in the mixed-wet systems, should they ever be obtained, will be lower than the  
188 reported values obtained in this work.

189 **Altering the Wetting State of the Rock.** After completing observations with the unaltered E1  
190 sample, an aging technique using crude oil was applied to change the wetting state of the core  
191 sample. An approach similar to Salathiel 1973<sup>24</sup> was performed by preparing a mixture of the  
192 evacuated crude oil with an organic precipitant, heptane. The addition of heptane induces the  
193 precipitation of asphaltene, leading to the alteration of the wetting state of mineral surfaces. Before  
194 aging the rock, observations were made with crude oil-heptane mixtures to identify ratios of fluid  
195 resulting in sufficient asphaltene precipitates to induce the wetting state change, but not so much  
196 that permeability of the rock core is significantly reduced. A detailed description is provided in the  
197 supporting information.

198 The core sample was fully saturated with evacuated brine and heated to 70 °C. A freshly made  
199 oil mixture of 28% evacuated Arabian Medium crude oil and 72% heptane was heated to 70 °C

200 and injected into the core sample for a total of 20 pore volumes with the direction of flow reversed  
201 midway to dynamically age the sample and speed the wetting alteration process<sup>36</sup>. The flow rates  
202 ranged from 0.1 ml min<sup>-1</sup> and up to 5 ml min<sup>-1</sup>. The sample was then left for further static aging  
203 (no flow) at 70 °C for 40 days. Then, the sample was cooled down to room temperature for at least  
204 24hrs. The oil mixture was displaced with 5 pore volumes of heptane injected at 10 ml min<sup>-1</sup> at  
205 room temperature. The core sample was then vacuum dried at 100 °C for three days to remove  
206 heptane and brine from the pore space by evaporating the fluids (heptane and water). Then the core  
207 sample was cooled to room temperature. Degassed deionized water was flushed into the sample  
208 for several pore volumes to remove salt that might have precipitated in the sample during drying.  
209 The sample was vacuum dried again at 70 °C for 12 hours to remove water. Finally, to ensure  
210 mobile oil was completely displaced, 5 pore volumes of CO<sub>2</sub> was injected at 20 MPa<sup>37</sup>. Next we  
211 performed the initial-residual core flood tests.

212 After completing the initial-residual core flooding experiments, the wetting properties of the  
213 mixed-wet (E1) and water-wet (E2) samples were measured by carrying out a standard Amott  
214 test<sup>29</sup> using Heptane and brine. Details of the test are provided in the supporting information. The  
215 Amott water ratio wettability index,  $\delta_w$ , was measured to be  $\delta_w = 0.48$  and  $\delta_w = 0.89$  for E1 and  
216 E2, respectively, after nine pore volumes of brine injected. The high  $\delta_w$  value of E2 is indicative  
217 of a strongly water-wet system where spontaneous imbibition leads to most of the oil in the sample  
218 displaced by water. On the other hand, spontaneous and forced imbibition produced comparable  
219 volumes of oil in the E1 sample resulting in a wettability index value similar to those measured in  
220 giant carbonate oil fields in the Middle East characterized as mixed-wet systems<sup>38</sup>. Additionally,  
221 the water-wet sample (E2) produced little oil after water breakthrough and quickly reached residual  
222 oil saturation. On the other hand, in the mixed-wet sample (E1) oil production continued for the

223 entire nine pore volumes of water injected, and likely would continue with continued brine  
224 injection. The displacement followed the pattern of a rapid desaturation with less than a single  
225 pore volume of brine injected, followed by a slow rate of desaturation with continued brine  
226 injection.

227 **Trapping Model.** A large number of models have been developed for describing the initial-  
228 residual relationship<sup>39</sup>. The Land model was used to fit the trapping data. It is one of the earliest  
229 and most widely used trapping models<sup>40</sup>. The residually trapped non-wetting phase saturation after  
230 imbibition,  $S_{CO_2,r}$  is an increasing function of the maximum non-wetting phase saturation achieved  
231 during drainage,  $S_{CO_2,i}$ ,

$$232 \quad S_{CO_2,r} = \frac{S_{CO_2,i}}{1 + CS_{CO_2,i}}, \quad (1)$$

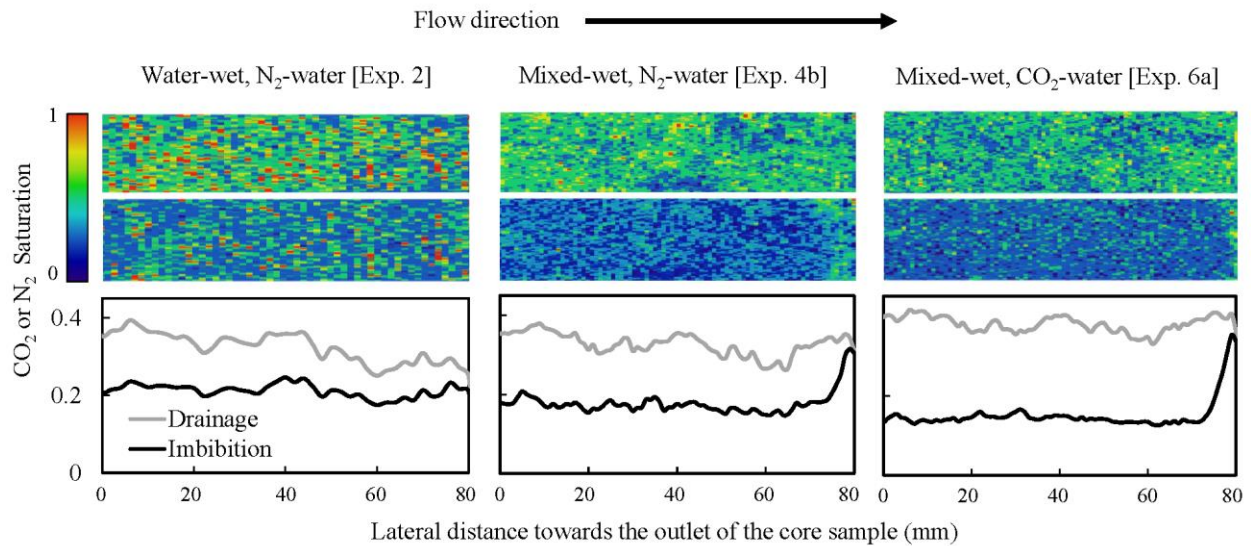
233 where  $C$  is a constant known as the Land coefficient and is equal to or greater than zero. Larger  
234 values of the constant indicate less trapping. Some models, e.g., the model of Spiteri et al. (2008)<sup>41</sup>  
235 have been proposed specifically for mixed-wet systems. In this case we found the Land model to  
236 fit our observations well. The data can in principle be fit using any of the alternatives.

237

## 238 RESULTS

239 Figure 1 shows examples of the slice average saturation along the rock core with corresponding  
240 two dimensional saturations maps of a central slice of the core for three of tests with high drainage  
241 flow rates. These graphs were generated for each experiment and used to quality check the results.  
242 The saturation maps show that CO<sub>2</sub> and N<sub>2</sub> were uniformly distributed in the core sample in central

243 parts of the core where the residual trapping was characterized, and not affected by mass transfer  
 244 or gravity segregation. The slice averaged saturations of the water-wet systems showed a declining  
 245 trend towards the outlet due to the capillary end effect. On the other hand, the saturation profiles  
 246 in the same rock sample after wetting state alteration exhibited an end-effect behavior, either with  
 247 no decline or increasing non-wetting phase saturation, characteristic of the mixed-wet state. The  
 248 drainage profiles were relatively uniform and saturation increased towards the outlet during  
 249 imbibition. Data from the central ~60 mm of the rock core were used to construct the initial-  
 250 residual curves to avoid the interference of the boundary affects.

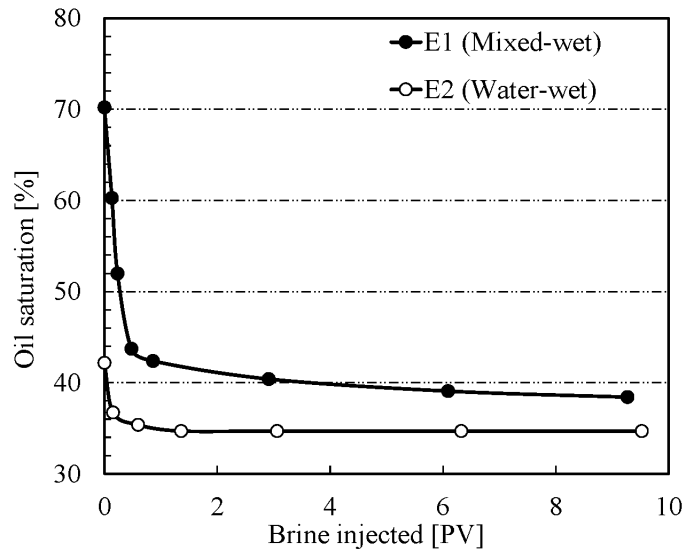


251

252 **Figure 1.** 2D saturation maps of the central slice of the core after drainage (top) and imbibition  
 253 (middle) for three experiments on the same sample. The core average saturation of the final section  
 254 of the core sample is shown in the lower graphs. The end-effect changes after the wettability  
 255 alteration.

256 In previous work it was confirmed that residual trapping in the water wet case was obtained  
 257 rapidly, with less than a pore volume of brine injected, and remained stable for more than 40 pore

258 volumes of subsequent brine injection<sup>34</sup>. In this work the initial rapid desaturation was again  
259 observed in tests with both the water wet and hydrocarbon altered rock. The subsequent stability  
260 of the residual saturation in the water-wet rock, and the slow and persistent desaturation of non-  
261 wetting phase in the altered rock, was then confirmed with the forced injection part of the Amott  
262 test shown in Figure 2.

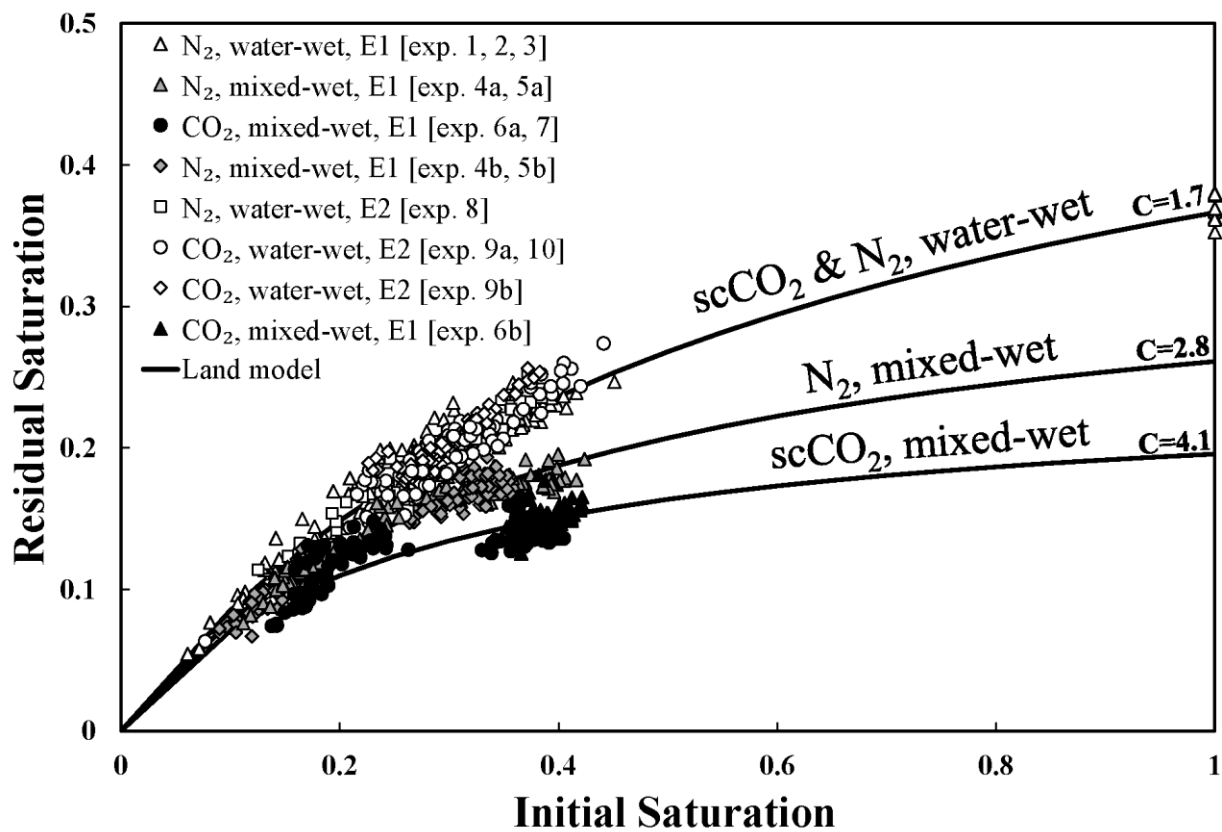


263

264 **Figure 2.** Results from the forced imbibition part of the Amott test showing oil saturation as a  
265 function of the pore volumes (PV) of brine injected, applied after 30 days of spontaneous  
266 imbibition. The water-wet sample (E1) produced little oil after water breakthrough while the  
267 mixed-wet sample (E2) continued oil production with a reducing remaining oil saturation trend  
268 as a function of PV injected.

269 Figure 3 shows initial-residual characteristic curves measured in this study with best fit curves  
270 using the Land model, Equation 1. Table 2 shows the best fit parameters for the Land hysteresis  
271 model. The trapping of CO<sub>2</sub> and N<sub>2</sub> in the unaltered samples, Experiments 1-3, 9-10, were  
272 indistinguishable, with best fit Land constants equivalent within the uncertainty bounds, Table 2.

273 This was consistent with earlier work<sup>34</sup> characterizing CO<sub>2</sub> trapping in unaltered sandstone rocks  
 274 and suggests that the wetting state is similar for the two systems<sup>16</sup>, but contrasts with observations  
 275 made using a different technique in which more trapping was observed for supercritical CO<sub>2</sub>  
 276 relative to gaseous CO<sub>2</sub> in an unaltered limestone<sup>11</sup>. The best fit Land constant for all of the data  
 277 (both CO<sub>2</sub> and N<sub>2</sub>) in the water wet tests was  $C = 1.73$ . At the highest initial saturations observed,  
 278 42% of the pore space, the residual saturation obtained was 24%.



279  
 280 **Figure 3.** Initial and residual CO<sub>2</sub> and N<sub>2</sub> saturations measured in this study. White symbols are  
 281 observations from the unaltered rock. Grey symbols are observations of N<sub>2</sub>-water from the mixed-  
 282 wet rock. Black symbols are observations of CO<sub>2</sub>-brine from the mixed-wet rock. The solid lines  
 283 show the best fit Land trapping model with their respective values for the parameterization

284 constant,  $C$ . The order of the experiments in the legend shows the sequence in which the  
 285 observations were made.

286 After alteration of the wetting state of the rock sample with the crude oil-heptane mixture, less  
 287 trapping was observed with both  $N_2$  and  $CO_2$ , Experiments 4-7. The value of the best fit Land  
 288 constant increased from 1.68 to 2.83 for  $N_2$  after 0.2 – 1.7 pore volumes of brine injected into the  
 289 core. The initial-residual relationship for  $N_2$  was obtained in repeated tests before (Experiments 4a  
 290 and 5a) and after (Experiments 4b and 5b) tests with  $CO_2$ . The data were indistinguishable, with  
 291 Land constants  $C = 2.86 \pm .06$  and  $2.80 \pm .06$  from the datasets obtained before and after exposure  
 292 of the altered rock to  $CO_2$ , respectively. This suggests that exposure to  $CO_2$  did not alter the wetting  
 293 state of the rock sample.

294 The trapping of  $CO_2$  was reduced even further compared to  $N_2$ . The best fit Land constant for  
 295  $CO_2$  increased to a value of 4.11 after 0.2 – 0.6 pore volumes of brine injected, with slow  
 296 desaturation continuing up to 1.6 pore volumes of injected brine (see the supporting information).  
 297 At the measured initial saturation of 42% the remaining  $CO_2$  was reduced to 15% compared with  
 298 19% for the  $N_2$  system. This observation was repeated with experiment 6b after exposure to  $N_2$ ,  
 299 showing both the precision in the measurement and that the rock core was not substantially altered  
 300 through multiple measurements obtained in the same sample.

301 **Table 2.** Best fit Land residual trapping hysteresis model coefficient

Experiment number	Wetting state	Trapped gas	$C^*$
1, 2, 8	water-wet	$N_2$	$1.68 \pm 0.05$
9a, 9b, 10	water-wet	$CO_2$	$1.74 \pm 0.05$
1, 2, 8, 9a, 9b, 10	water-wet	$CO_2, N_2$	$1.73 \pm 0.03$
4a, 4b, 5a, 5b	mixed-wet	$N_2$	$2.83 \pm 0.04$



302                    6a, 6b, 7                    mixed-wet                     $CO_2$                      $4.11 \pm 0.08$   
\*  $C$  values  $\pm$  error calculated as two times the standard deviation of best fit  $C$

303

304        DISCUSSION

305        The results for the unaltered rocks show the same degree of trapping for  $CO_2$  and  $N_2$ . The Land  
306        constant is larger, indicating less trapping, than values obtained characterizing  $CO_2$  trapping in  
307        Berea sandstone<sup>2</sup>. The source of the difference may be due to pore structure and/or wetting state  
308        differences<sup>2</sup>, although the similarity of the  $N_2$  and  $CO_2$  observations in this study suggests pore  
309        structure differences to be the likely explanation. The equivalence of the  $CO_2$  and  $N_2$  is consistent  
310        with past observations with Berea sandstone<sup>34</sup>, but contrasts with observations made in a different  
311        carbonate rock in which more trapping was observed for supercritical  $CO_2$  as compared with  
312        gaseous  $CO_2$  in a different carbonate rock<sup>11</sup>. The contrasting results could be due to differences in  
313        rock structure leading to different sensitivities to contact angle changes, or experimental  
314        procedure, and is discussed further below.

315        In the mixed-wet sample the trapping of  $N_2$  and  $CO_2$  systems were significantly less than the  
316        trapping in the unaltered rocks. As discussed in the introduction, this result was consistent with  
317        past observations evaluating the impact of the mixed-wet state on the capillary trapping of  
318        hydrocarbon liquids<sup>23-25,42</sup>. This is generally thought to result from oil-wet surfaces providing  
319        connected pathways for thin film drainage of non-polar fluids<sup>24,40</sup>.

320        The trapping was also specific to the fluid pair, with less  $CO_2$  remaining in the pore space than  
321         $N_2$  upon secondary imbibition. The observations with  $N_2$  and  $CO_2$  were alternated and repeated  
322        with the same result, indicating that the difference was not due to chemical reaction between the

323 fluids and the rock, or altered wetting surfaces. This suggests that the difference was due to the  
324 impact of a difference in contact angle between the CO<sub>2</sub>-brine and N<sub>2</sub>-water on the surfaces with  
325 an altered wetting state, with the CO<sub>2</sub> more wetting of the altered surfaces than N<sub>2</sub>.

326 This response is predicted by theoretical considerations of contact angles on smooth surfaces<sup>43</sup>.  
327 With a contact angle,  $\theta$  [rad], measured in the aqueous phase, the relationship between the CO<sub>2</sub>-  
328 brine and N<sub>2</sub>-brine angles are dependent on the ratio of their respective values of interfacial tension,  
329  $\sigma$ , [mN/m], through the relationship  $\cos \theta_{CO_2-w} \propto \frac{\sigma_{N_2-w}}{\sigma_{CO_2-w}} \cos \theta_{N_2-w}$ . A derivation is included in  
330 the supporting information. The interfacial tension of N<sub>2</sub> and gaseous CO<sub>2</sub> systems are much larger  
331 than that of the supercritical CO<sub>2</sub> system<sup>30,31</sup>, predicting a larger contact angle for CO<sub>2</sub> (more CO<sub>2</sub>-  
332 wetting) on oil-wet surfaces and smaller contact angles for CO<sub>2</sub> (less CO<sub>2</sub>-wetting) on water-wet  
333 surfaces.

334 In practice, small changes in contact angle do not usually manifest in changes in flow properties  
335 due to the counterbalancing effects of pore structure and mineral roughness<sup>20,21</sup>. The differences  
336 in how this is manifest in trapping in the water-wet (equivalent CO<sub>2</sub> and N<sub>2</sub> trapping) and mixed-  
337 wet (less CO<sub>2</sub> trapping) states may be due to the values of the contact angles (the pore scale force  
338 balance changes as  $\frac{d(\cos \theta)}{d\theta} = -\sin \theta$ ), or due to mineral wall roughness smoothed out by  
339 asphaltene deposition in the mixed-wet rock. It is notable that the difference in trapping of gaseous  
340 and supercritical CO<sub>2</sub> observed in an unaltered carbonate in El-Maghraby and Blunt (2012)<sup>11</sup> also  
341 follows the theoretical argument. Thus it is possible that the difference between those observations  
342 and the observations in unaltered rock reported here are not contradictory, but rather due to a  
343 difference in sensitivity of the flow properties to changes in contact angle in the respective rocks.

344 Finally, the decreased trapping values obtained in the altered rocks are conservative – it is likely  
345 that the irreducible residual saturation is lower. The Amott test indeed showed continued slow  
346 desaturation of the non-wetting phase with continued brine flooding of the core. It is evident that  
347 the residual trapping of CO<sub>2</sub> in mixed-wet carbonate reservoirs will be significantly less than in  
348 reservoir units that have not been exposed to hydrocarbon.

349

## 350 IMPLICATIONS

351 On the one hand, there are a number of attributes of the use of commercial oil fields that  
352 contribute significantly to the safety and success of storage projects. The fields are well  
353 characterized. The fields also have a demonstrated fluid trap and are not as dependent on capillary  
354 and dissolution trapping as the majority of CO<sub>2</sub> storage sites<sup>13,14</sup>.

355 On the other hand, it is important that large scale assessments, e.g., of storage capacity take into  
356 account the difference in flow physics controlling storage in oil fields relative to those of saline  
357 aquifers. A simple example using the analytic model of Juanes et al. 2010<sup>44</sup> illustrates the  
358 significance of the weakened capillary trapping for CO<sub>2</sub> flow at the regional scale. Consider a  
359 depleted oil reservoir with a thickness of 100 m with the same petrophysical properties of the  
360 Estailades limestone used in this study – a permeability and porosity of 138 md and 0.28,  
361 respectively. The model was used to estimate the ultimate footprint of a CO<sub>2</sub> plume migrating  
362 horizontally below a confining caprock layer, and the timescale required for immobilization  
363 through capillary trapping. Consider 100 Mt of CO<sub>2</sub> injected every year using 100 wells, with an  
364 interwell spacing of 1 km, for a period of 5 years. The connate water saturation and  $k_{rg}$  was  
365 assumed to be 0.4 and 0.6, respectively<sup>45</sup>. The model accounts for gravity override, capillary

366 trapping, natural groundwater flow, and the shape of the plume during the injection period but  
367 does not account for reservoir heterogeneity and changes to relative permeability due to changes  
368 in the wetting state.

369 In the water wet system, an initial CO<sub>2</sub> saturation of 42% corresponded to a 24% residual  
370 saturation. This resulted in a migration of the plume ~ 50 km prior to immobilization in ~ 5,000  
371 years. For the same initial CO<sub>2</sub> saturation, only 15% was trapped in the mixed-wet system,  
372 corresponding to a migration path of ~ 130 km and immobilization in ~ 16,000 years.

373 Our results show that one of the key processes for maximizing CO<sub>2</sub> storage capacity and security  
374 is significantly weakened in many hydrocarbon reservoirs relative to saline aquifers. We anticipate  
375 this work to highlight a key issue for the early deployment of carbon storage – that those sites  
376 which are economically most appealing as initial project opportunities are the very locations in  
377 which the contribution of capillary trapping to storage security will be minimized. This should  
378 serve as a starting point for modelling studies to incorporate the reduced impact of capillary  
379 trapping on CO<sub>2</sub> injection projects using hydrocarbon reservoirs.

380

381 ASSOCIATED CONTENT

382 **Supporting Information.** Tables listing all IR results and corresponding 2D saturation maps of  
383 all tests are included. Derivation of the relationship between contact angles. Further information  
384 on experimental procedures, porosity and saturation measurements, a schematic of the  
385 coreflooding rig, asphaltene precipitation measurement, wetting alteration procedure, wetting  
386 state assessment, rock samples, remaining CO<sub>2</sub> saturations as a function of pore volume injected

387 of brine in mixed-wet system. This material is available free of charge via the Internet at  
388 <http://pubs.acs.org>.

389

## 390 AUTHOR INFORMATION

### 391 **Corresponding Author**

392 \*E-mail: [a.al-menhali12@imperial.ac.uk](mailto:a.al-menhali12@imperial.ac.uk)

### 393 **Author Contributions**

394 The manuscript was written through contributions of all authors. All authors have given approval  
395 to the final version of the manuscript.

### 396 **Notes**

397 The authors declare no competing financial interest.

398

## 399 ACKNOWLEDGMENT

400 We gratefully acknowledge funding from the Qatar Carbonates and Carbon Storage Research  
401 Centre (QCCSRC), provided jointly by Qatar Petroleum, Shell, and Qatar Science & Technology  
402 Park.

403 We thank Professor Martin Blunt for helpful discussions about the wetting state alteration and  
404 observed responses of the residual trapping characteristic curves.

405 The authors wish to thank the Editors and four anonymous reviewers which provided thoughtful  
406 comments and analysis on earlier drafts of this work.

407

408 ABBREVIATIONS

409 CO<sub>2</sub> carbon dioxide

410 N<sub>2</sub> Nitrogen

411 *C* Land model coefficient

412 sc supercritical

413

414 REFERENCES

415 1. Pachauri, R. K.; Allen, M.; Barros, V.; Broome, J.; Cramer, W.; Christ, R.; Church, J.;  
416 Clarke, L.; Dahe, Q.; Dasgupta, P., Climate Change 2014: Synthesis Report. Contribution of  
417 Working Groups I, II and III to the Fifth Assessment Report. *Intergovernmental Panel on Climate*  
418 *Change*. **2014**. 151.

419 2. Krevor, S.; Blunt, M. J.; Benson, S. M.; Pentland, C. H.; Reynolds, C.; Al-Menhali, A.;  
420 Niu, B., Capillary trapping for geologic carbon dioxide storage – From pore scale physics to field  
421 scale implications. *International Journal of Greenhouse Gas Control* **2015**, *40*, 221-237.

422 3. Hesse, M.; Orr, F.M. Jr.; Tchelepi, H., Gravity currents with residual trapping. *Journal of*  
423 *Fluid Mechanics* **2008**, *611*, 35-60.

424 4. Juanes, R.; Spiteri, E. J.; Orr, F.M. Jr.; Blunt, M. J., Impact of relative permeability  
425 hysteresis on geological CO<sub>2</sub> storage. *Water Resources Research* **2006**, *42* (12).  
426 DOI:10.1029/2005WR004806.

- 427 5. Warwick, P. D., M. S. Blondes, S. T. Brennan, M. L. Buursink, S. M. Cahan, J. L.;  
428 Coleman, T. A. C., M. D. Corum, J. A. Covault, W. H. Craddock, C. A. DeVera,; C. Doolan, R.  
429 M. D. I., L. J. Drew, J. A. East, P. A. Freeman, C. P. Garrity, K. J.; Gooley, M. A. G., H.  
430 Jahediesfanjani, C. D. Lohr, J. C. Mars, M. D. Merrill, R. A.; Olea, T. L. R.-A., W. A. Rouse, P.  
431 G. Schruben, J. H. Schuenemeyer, E. R.; Slucher, B. A. V., M. K. Verma, National assessment of  
432 geologic carbon dioxide storage resources - Results. *U.S. Geological Survey* **2013**, (1386), 41.
- 433 6. Szulczewski, M. L.; MacMinn, C. W.; Herzog, H. J.; Juanes, R., Lifetime of carbon capture  
434 and storage as a climate-change mitigation technology. *Proceedings of the National Academy of*  
435 *Sciences* **2012**, *109* (14), 5185-5189.
- 436 7. Gammer, D.; Smith, G.; Green, A., The Energy Technology Institute's UK CO<sub>2</sub> Storage  
437 Appraisal Project (UKSAP). *Society of Petroleum Engineers* **2011**, 148426.
- 438 8. Halland, E. K., I. T. Gjeldvik, W. T. Johansen, C. Magnus, I. M. Meling, S. Pedersen,; F.  
439 Riis, T. S., I. Tappel, CO<sub>2</sub> Storage Atlas Norwegian North Sea. *The Norwegian Petroleum*  
440 *Directorate* **2011**. Available at: [http://www.npd.no/Global/Norsk/3-](http://www.npd.no/Global/Norsk/3-Publikasjoner/Rapporter/PDF/CO2-ATLAS-lav.pdf)  
441 [Publikasjoner/Rapporter/PDF/CO<sub>2</sub>-ATLAS-lav.pdf](http://www.npd.no/Global/Norsk/3-Publikasjoner/Rapporter/PDF/CO2-ATLAS-lav.pdf)
- 442 9. Doughty, C., Modeling geologic storage of carbon dioxide: Comparison of non-hysteretic  
443 and hysteretic characteristic curves. *Energy Conversion and Management* **2007**, *48* (6), 1768-  
444 1781.
- 445 10. Qi, R.; LaForce, T. C.; Blunt, M. J., Design of carbon dioxide storage in aquifers.  
446 *International Journal of Greenhouse Gas Control* **2009**, *3* (2), 195-205.

- 447 11. El-Maghraby, R. M.; Blunt, M. J., Residual CO<sub>2</sub> Trapping in Indiana Limestone.  
448 *Environmental science & technology* **2013**, *47* (1), 227-233.
- 449 12. Benson, S. M.; Bennaceur, K.; Cook, P.; Davison, J.; de Coninck, H.; Farhat, K.; Ramirez,  
450 A.; Simbeck, D.; Surles, T.; Verma, P.; Wright, I., Chapter 13 - Carbon Capture and Storage. In  
451 *Global Energy Assessment - Toward a Sustainable Future*, Cambridge University Press,  
452 Cambridge, UK and New York, NY, USA and the International Institute for Applied Systems  
453 Analysis, Laxenburg, Austria, **2012**, 993-1068.
- 454 13. Haszeldine, R. S., Carbon Capture and Storage: How Green Can Black Be? *Science* **2009**,  
455 *325* (5948), 1647-1652.
- 456 14. Herzog, H.; Golomb, D., Carbon capture and storage from fossil fuel use. *Encyclopedia of*  
457 *energy* **2004**, *1*, 1-11.
- 458 15. Tomski, P., Carbon capture and storage: a vital low carbon technology that can deliver on  
459 economic development, energy security, and climate goals. *Global CCS Institute report* **2015**.
- 460 16. Al-Menhali, A.; Niu, B.; Krevor, S., Capillarity and wetting of carbon dioxide and brine  
461 during drainage in Berea sandstone at reservoir conditions. *Water Resources Research* **2015**, *51*  
462 (10), 7895-7914. DOI:10.1002/2015WR016947.
- 463 17. Iglauer, S.; Pentland, C. H.; Busch, A., CO<sub>2</sub> wettability of seal and reservoir rocks and the  
464 implications for carbon geo-sequestration. *Water Resources Research* **2015**, *51* (1), 729-774.
- 465 18. Wang, S.; Tokunaga, T. K., Capillary Pressure–Saturation Relations for Supercritical CO<sub>2</sub>  
466 and Brine in Limestone/Dolomite Sands: Implications for Geologic Carbon Sequestration in  
467 Carbonate Reservoirs. *Environmental Science & Technology* **2015**, *49* (12), 7208-7217.



- 468 19. Kovscek, A. R.; Wong, H.; Radke, C. J., A pore-level scenario for the development of  
469 mixed wettability in oil reservoirs. *AIChE Journal* **1993**, *39* (6), 1072-1085.
- 470 20. Anderson, W. G., Wettability Literature Survey - Part 4: Effects of Wettability on Capillary  
471 Pressure. *Journal of Petroleum Technology* **1987**, *39* (10), 1283-1300.
- 472 21. Anderson, W. G., Wettability Literature Survey - Part 5: The Effects of Wettability on  
473 Relative Permeability. *Journal of Petroleum Technology* **1987**, *39* (11), 1453-1468.
- 474 22. Anderson, W. G., Wettability Literature Survey - Part 6: The Effects of Wettability on  
475 Waterflooding. *Journal of Petroleum Technology* **1987**, *39* (12), 1605-1622.
- 476 23. Chilingar, G. V.; Yen, T., Some notes on wettability and relative permeabilities of  
477 carbonate reservoir rocks, II. *Energy Sources* **1983**, *7* (1), 67-75.
- 478 24. Salathiel, R. A., Oil Recovery by Surface Film Drainage in Mixed-Wettability Rocks.  
479 *Journal of Petroleum Technology* **1973**, *25* (10), 1,216-1,224.
- 480 25. Tanino, Y.; Blunt, M. J., Laboratory investigation of capillary trapping under mixed-wet  
481 conditions. *Water Resources Research* **2013**, *49* (7), 4311-4319.
- 482 26. Roehl, P. O.; Choquette, P. W., *Carbonate petroleum reservoirs*. Springer Science &  
483 Business Media: New York, **1985**.
- 484 27. Akbar, M.; Vissapragada, B.; Alghamdi, A. H.; Allen, D.; Herron, M.; Carnegie, A.; Dutta,  
485 D.; Olesen, J.-R.; Chourasiya, R.; Logan, D., A snapshot of carbonate reservoir evaluation. *Oilfield*  
486 *Review* **2000**, *12* (4), 20-21.

- 487 28. Le Guen, Y.; Renard, F.; Hellmann, R.; Brosse, E.; Collombet, M.; Tisserand, D.; Gratier,  
488 J. P., Enhanced deformation of limestone and sandstone in the presence of high  $P_{CO_2}$  fluids.  
489 *Journal of Geophysical Research: Solid Earth* **2007**, *112* (B5). DOI: 10.1029/2006JB004637.
- 490 29. Amott, E., Observations relating to the wettability of porous rock. *Trans. AIME* **1959**, *216*,  
491 156–162.
- 492 30. Li, X.; Boek, E.; Maitland, G. C.; Trusler, J. P. M., Interfacial Tension of (Brines +  $CO_2$ ):  
493 (0.864 NaCl + 0.136 KCl) at Temperatures between (298 and 448) K, Pressures between (2 and  
494 50) MPa, and Total Molalities of (1 to 5)  $mol \cdot kg^{-1}$ . *Journal of Chemical & Engineering Data* **2012**,  
495 *57* (4), 1078-1088.
- 496 31. Yan, W.; Zhao, G.-Y.; Chen, G.-J.; Guo, T.-M., Interfacial Tension of (Methane +  
497 Nitrogen) + Water and (Carbon Dioxide + Nitrogen) + Water Systems. *Journal of Chemical &*  
498 *Engineering Data* **2001**, *46* (6), 1544-1548.
- 499 32. Kestin, J.; Khalifa, H. E.; Correia, R. J., Tables of the dynamic and kinematic viscosity of  
500 aqueous NaCl solutions in the temperature range 20-150 °C and the pressure range 0.1-35 MPa.  
501 *American Chemical Society and the American Institute of Physics for the National Bureau of*  
502 *Standards*: **1981**. 10 (10), 71-88.
- 503 33. Lemmon, E.; McLinden, M.; Friend, D., Thermophysical Properties of Fluid Systems in  
504 NIST Chemistry webbook; NIST Standard Reference Database No. 69, Eds. P. Linstrom and W.  
505 Mallard, National Institute of Standards and Technology, Gaithersburg MD, 20899,  
506 <http://webbook.nist.gov>. Retrieved **May 6, 2013**.

- 507 34. Niu, B.; Al-Menhali, A.; Krevor, S., The impact of reservoir conditions on the residual  
508 trapping of carbon dioxide in Berea sandstone. *Water Resources Research* **2015**, 51 (4), 2009-  
509 2029. DOI:10.1002/2014WR016441.
- 510 35. Akin, S.; Kovscek, A., Computed tomography in petroleum engineering research.  
511 *Geological Society, London, Special Publications* **2003**, 215 (1), 23-38.
- 512 36. Fernø, M.; Torsvik, M.; Haugland, S.; Graue, A., Dynamic laboratory wettability  
513 alteration. *Energy & Fuels* **2010**, 24 (7), 3950-3958.
- 514 37. Amro, M.; Freese, C.; Finck, M.; Jaeger, P., Effect of CO<sub>2</sub>-miscibility in EOR. *Society of*  
515 *Petroleum Engineers* **2015**, 172705.
- 516 38. Okasha, T. M.; Funk, J. J.; Rashidi, H. N., Fifty Years of Wettability Measurements in the  
517 Arab-D Carbonate Reservoir. *Society of Petroleum Engineers* **2007**, 105114.
- 518 39. Pentland, C. H.; Itsekiri, E.; Al-Mansoori, S.; Iglauer, S.; Bijeljic, B.; Blunt, M. J.,  
519 Measurement of Nonwetting-Phase Trapping in Sandpacks. *SPE Journal* **2010**, 15 (02), 274-281.
- 520 40. Land, C. S., Calculation of Imbibition Relative Permeability for Two- and Three-Phase  
521 Flow from Rock Properties. *Society of Petroleum Engineers* **1968**, 8 (2), 149-156.
- 522 41. Spiteri, E. J.; Juanes, R.; Blunt, M. J.; Orr, F.M. Jr., A New Model of Trapping and Relative  
523 Permeability Hysteresis for All Wettability Characteristics. *Society of Petroleum Engineers* **2008**,  
524 13 (3), 277-288.
- 525 42. Jadhunandan, P. P.; Morrow, N. R., Effect of Wettability on Waterflood Recovery for  
526 Crude-Oil/Brine/Rock Systems. *SPE Reservoir Engineering* **1995**, 10 (01), 40-46.

- 527 43. Blunt, M. J., Constraints on Contact Angles for Multiple Phases in Thermodynamic  
528 Equilibrium. *Journal of Colloid and Interface Science* **2001**, 239 (1), 281-282.
- 529 44. Juanes, R.; MacMinn, C.; Szulczewski, M., The Footprint of the CO<sub>2</sub> Plume during Carbon  
530 Dioxide Storage in Saline Aquifers: Storage Efficiency for Capillary Trapping at the Basin Scale.  
531 *Transp Porous Med* **2010**, 82 (1), 19-30.
- 532 45. Bennion, D. B.; Bachu, S., Supercritical CO<sub>2</sub> and H<sub>2</sub>S - Brine Drainage and Imbibition  
533 Relative Permeability Relationships for Intercrystalline Sandstone and Carbonate Formations.  
534 *Society of Petroleum Engineers* **2006**, 99326.